AIAA JOURNAL
Vol. 37, No. 1, January 1999

Analytical and Finite Element Modeling of Riveted Lap Joints in Aircraft Structure

Y. Xiong* and O. K. Bedair†
National Research Council Canada, Ottawa, Ontario K1A 0R6, Canada

Modeling procedures, using both analytical and numerical methods, for the stress analysis of riveted lap joints in aircraft structure are proposed. In the analytical method, a complex variational approach is employed to determine the stresses in joined plates containing single or multiple loaded holes. The effects of finite geometry are taken into account by the variational formulations. An iterative scheme is carried out to handle the deformation compatibility between all joined members. In the numerical method, finite element analyses are conducted using the commercial packages MSC/PATRAN and MSC/NASTRAN. Gap elements are used to simulate the rivet–hole interactions. Both linear and nonlinear deformations are considered. The two modeling procedures are complementary to each other. Whereas the analytical method is efficient for parametric studies, the numerical method is capable of dealing with relatively more complicated geometry and loading conditions. Results of several example problems are presented, and a good agreement between the two modeling procedures is demonstrated.

Nomenclature

A_{ij}	= in-plane stiffness coefficients
N_r, N_θ, $N_{r\theta}$	= stress components with respect to cylindrical system defined at rivet hole
N_x, N_y, N_{xy}	= stress components with respect to x–y coordinate system
P	= external load applied to joint
P_i	= ith rivet load in joint
P_r^i	= pressurized stress at the ith rivet hole
p_1, p_2	= two complex constants in calculating displacement component u
q_1, q_2	= two complex constants in calculating displacement component v
r_i	= radius of the ith rivet hole
u, v	= displacement components with respect to x–y coordinate system
u_r, u_θ	= displacement components with respect to cylindrical system at rivet hole
$\bar{u}_r^i$	= specified radial displacement components of the ith rivet hole edge
z_1, z_2	= two complex coordinate variables
β	= positional angle along each rivet hole edge
ζ_{ki}	= conformal mapping functions
$\lambda^i(\beta)$	= Lagrangian multiplier for the ith rivet hole
μ_1, μ_2	= two complex roots with positive imaginary part of the characteristic equation
φ_1, φ_2	= two complex stress functions

Introduction

RIVETED lap joints, made of metallic and composite materials, are structural components commonly used for assembly of parts in aircraft structures. The current economical climate requires that both military and civilian aircraft be operated beyond their design lives. Therefore, maintenance and repair are important issues to be investigated for aging aircraft structure.[1] Research programs have been underway at the Institute for Aerospace Research of the National Research Council Canada on bolted patch repair of damaged composite skin panels[2] and multiple site damage of lap splice joints.[3] A main task in the research programs is to develop efficient modeling procedures for mechanically fastened composite joints and riveted lap joints in aircraft fuselage structure. Both analytical and numerical methods are to be examined. This is challenging work because of the complex geometry and load transfer in the joints. An important consideration about the modeling procedures is to maintain a good balance between accuracy and the computational efficiency. In the following discussion, the geometry and configuration of the two types of joints are idealized as two plates joined together by frictionless rivets without distinguishing the differences in geometry.

Various analytical approaches following Lekhnitskii[4] have been developed for composite joints.[5,6] These approaches are based on an infinite plate assumption. Finite width correction factors are required when applying the analytical approaches to finite sized plates.[7] These correction factors, in most cases, are developed based on finite element analyses. This requirement of using a numerical technique to generate correction factors makes the Lekhnitskii complex potential based analytical approaches less suitable for designing complex joint configurations. In addition, the closed-form solutions are valid for pure bearing loading only.

To eliminate the requirement for finite width correction factors, the analytical solutions involving complex stress potentials have been employed in different fashions. The boundary collocation method was used for crack problems[8] and contact problems.[9] This method involves a conformal mapping and a least-squares scheme. A hybrid method in conjunction with complex stress functions was formulated for aircraft panels with multiple site damage near the rivet holes.[10] More recently, a mixed form of the complex variational approach was developed for composite joints containing multiple rivet holes under a unidirectional load.[11]

In addition to the analytical approaches, numerical methods have been widely used for both composite joints and metallic lap joints. Two-dimensional finite element analyses with assumed distribution of rivet loads were conducted for strength prediction of composite joints.[12–14] Finite element analyses were also carried out for metallic lap joints in different ways such as a two-dimensional model with merged nodes,[15] a two-dimensional model with assumed displacement boundary conditions,[16] and a three-dimensional model with interface or gap elements.[17,18] Although the three-dimensional analyses can provide more accurate stress predictions, particularly for locations around rivet holes, extensive modeling efforts and computer time are required. This approach often limits modeling to only a small number of rivet holes. In the present work, two-dimensional finite element models have been developed for rivet lap joints using

Received April 10, 1998; revision received Aug. 12, 1998; accepted for publication Sept. 8, 1998.

*Research Officer, Structures, Materials, and Propulsion Laboratory, Institute for Aerospace Research. Member AIAA.

†Postdoctoral Fellow, Structures, Materials, and Propulsion Laboratory, Institute for Aerospace Research.

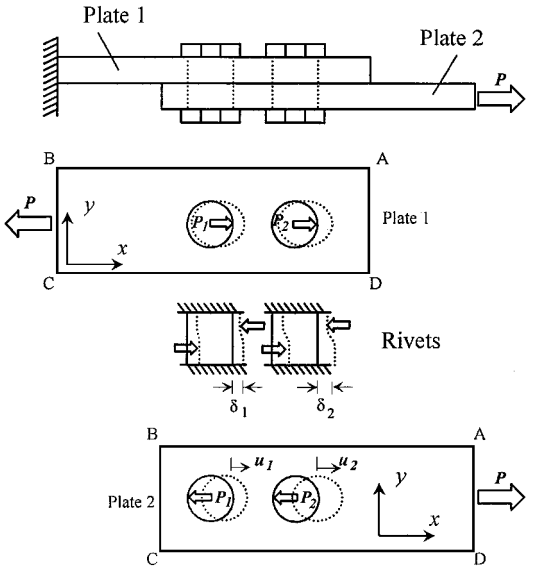

Fig. 1 Configuration of two-rivet lap joint.

gap elements to simulate the rivet–hole interactions. The effects of the number of gap elements are examined from the point of view of accuracy and computational efficiency.

In this paper, the development of the analytical and numerical modeling procedures for lap joints involving single and multiple rivet holes is described. Detailed results for several example problems of lap joints under the unidirectional loading condition are presented and discussed. The two modeling procedures are complementary to each other and demonstrate a reasonably good agreement between the results from the two modeling procedures.

Statement of Problem

The problem under study in this paper is a single shear lap joint, which involves two composite or metallic plates joined by single or multiple rivets, as shown in Fig. 1 for a joint with two rivets. In analytical modeling, the two plates are treated, in general, as anisotropic plates because the isotropic metallic plate can be represented as a special case. The two plates are of the same finite width, and they have, in general, m circular loaded holes of various sizes that are arbitrarily located. The tensile load P applied at the edge of the lower plate (plate 2) is in equilibrium with the m rivet loads, P_i ($i = 1, 2, \ldots, m$). This load is transferred to the upper plate (plate 1).

It is noted that the actual stress state at the rivet location is complex and three dimensional in nature. To develop relatively simple modeling methods with reasonable accuracy, we made some assumptions in this work: 1) the load on one plate is transferred by flexible frictionless rivets over half of the hole edges, and 2) the secondary bending of the plates due to load eccentricity is negligible compared with the in-plane deformations. Therefore the two plates are assumed to be in a plane stress state and the rivets are modeled as elastic beams with appropriate end conditions.

Analytical Modeling Method

Iterative Scheme

As seen in Fig. 1, the external load P applied on plate 2 is transferred by the rivets to plate 1. This load transfer results in the deflection of rivets and the elongation of the holes in the upper plate. To consider the deformation compatibility between the jointed members, we established an iterative scheme that involves the following steps for joint stress analysis:

1) Assign initial values for rivet loads that are in equilibrium with the externally applied load P.

2) Calculate the hole elongation in plate 1 under the applied load and the rivet loads. The rivet loads are simulated by a cosine function.

3) Calculate the deflections of the rivets under the shear loads transferred by the rivets.

4) Calculate the summation of the hole elongations and rivet deflections in plate 1. The combined deformation is taken as the rigid-body movement of the contact region of the corresponding rivet holes in plate 2. Calculate the reactions on holes of plate 2 under the rigid body motions and the applied load P.

5) Take the reactions on the holes of plate 2 as new rivet loads and repeat steps 2–4 until a convergent solution is obtained.

Variational Formulations for Plates 1 and 2

Because the two plates are in a plane stress state, the theories of two-dimensional anisotropic elasticity are applied to the stress analysis of the two plates. That is, two complex stress potentials are used to derive the stress and displacement components. For the sake of simplicity, identical sets of notations are employed for the two plates and the basic equations are written as

$$N_x = 2\,\mathrm{Re}\left[\mu_1^2\frac{\mathrm{d}\varphi_1(z_1)}{\mathrm{d}z_1} + \mu_2^2\frac{\mathrm{d}\varphi_2(z_2)}{\mathrm{d}z_2}\right]$$
$$N_y = 2\,\mathrm{Re}\left[\frac{\mathrm{d}\varphi_1(z_1)}{\mathrm{d}z_1} + \frac{\mathrm{d}\varphi_2(z_2)}{\mathrm{d}z_2}\right] \tag{1}$$
$$N_{xy} = -2\,\mathrm{Re}\left[\mu_1\frac{\mathrm{d}\varphi_1(z_1)}{\mathrm{d}z_1} + \mu_2\frac{\mathrm{d}\varphi_2(z_2)}{\mathrm{d}z_2}\right]$$

$$u = 2\,\mathrm{Re}[p_1\varphi_1(z_1) + p_2\varphi_2(z_2)]$$
$$v = 2\,\mathrm{Re}[q_1\varphi_1(z_1) + q_2\varphi_2(z_2)] \tag{2}$$

Plate 1 is under the applied load P and rivet loads P_i. The rivet loads cause a stress due to pressure against the right half of the hole edge, and this stress is assumed to have a cosine distribution as

$$P_r^i(\beta) = (2P_i/\pi r_i)\cos\beta \tag{3}$$

Because plate 1 does not have any displacement boundary conditions, the minimum potential energy theorem is applied. The total potential energy of plate 1 is written as

$$\begin{aligned}\tilde{\Pi}_1 = {} & \frac{1}{2}\int_\Omega\left[A_{11}\left(\frac{\partial u}{\partial x}\right)^2 + 2A_{12}\frac{\partial u}{\partial x}\frac{\partial v}{\partial y} + A_{22}\left(\frac{\partial v}{\partial y}\right)^2\right.\\ & + 2\left(A_{16}\frac{\partial u}{\partial x} + A_{26}\frac{\partial u}{\partial x}\right)\left(\frac{\partial u}{\partial y} + \frac{\partial v}{\partial x}\right)\\ & \left. + A_{66}\left(\frac{\partial u}{\partial y} + \frac{\partial v}{\partial x}\right)^2\right]\mathrm{d}x\,\mathrm{d}y - \int_{y_B}^{y_C}\frac{P}{W}u|_{x=-L/2}\,\mathrm{d}y\\ & - \sum_{i=1}^{m}\int_{-\pi/2}^{\pi/2}p_r^i(\beta)u_r(\beta)r_i\,\mathrm{d}\beta\end{aligned} \tag{4}$$

where Ω denotes the domain, L the length, and W the width of the plate.

Using the integration by parts, the first-order variation of the preceding energy functional with respect to u and v, respectively, is derived and written as

$$\begin{aligned}\delta\tilde{\Pi}_1 = {} & -\int_{x_A}^{x_B}(N_{xy}\delta u + N_y\delta v)|_{y=W/2}\,\mathrm{d}x\\ & + \int_{y_B}^{y_C}\left[\left(N_x - \frac{P}{W}\right)\delta u + N_{xy}\delta v\right]|_{x=-L/2}\,\mathrm{d}y\\ & - \int_{x_C}^{x_D}(N_{xy}\delta u + N_y\delta v)|_{y=-W/2}\,\mathrm{d}x\\ & + \int_{y_D}^{y_A}(N_x\delta u + N_{xy}\delta v)|_{x=-L/2}\,\mathrm{d}y\\ & - \sum_{i=1}^{m}\left\{\int_{-\pi/2}^{\pi/2}\left[(N_r^i - p_r^i)\delta u_r^i + N_{r\theta}^i\delta u_\theta^i\right]r_i\,\mathrm{d}\beta\right.\\ & \left. + \int_{\pi/2}^{3\pi/2}(N_r^i\delta u_r^i + N_{r\theta}^i\delta u_\theta^i)r_i\,\mathrm{d}\beta\right\}\end{aligned} \tag{5}$$

where the stress components are related to the displacement components by the constitutive equations. In addition, the area integrations, in Eq. (5), which are associated with the two equilibrium equations, are eliminated because of the automatic satisfaction by using the stress potentials. Therefore the variational formulation involves only boundary integrations, which are associated with the boundary conditions.

For plate 2, which has both force and displacement boundary conditions, a mixed variational formulation is established. The energy functional in this case is written as

$$\tilde{\Pi}_2 = \frac{1}{2}\int_\Omega \left[A_{11}\left(\frac{\partial u}{\partial x}\right)^2 + 2A_{12}\frac{\partial u}{\partial x}\frac{\partial v}{\partial y} + A_{22}\left(\frac{\partial v}{\partial y}\right)^2 + 2\left(A_{16}\frac{\partial u}{\partial x} + A_{26}\frac{\partial u}{\partial x}\right)\left(\frac{\partial u}{\partial y} + \frac{\partial v}{\partial x}\right) + A_{66}\left(\frac{\partial u}{\partial y} + \frac{\partial v}{\partial x}\right)^2 \right] dx\, dy - \int_{y_D}^{y_A} \frac{P}{W} u|_{x=-L/2}\, dy + \sum_{i=1}^{m} \int_{\pi/2}^{3\pi/2} \lambda^i(\beta)\left[u_r(\beta) - \bar{u}_r^i\right] r_i\, d\beta \tag{6}$$

where $\lambda^i(\beta)$ represents the compressive stress against the left half of the hole edge caused by the rivet load. In a similar way, the first-order variation of the preceding energy functional with respect to u, v, and λ^i, respectively, is derived and written as

$$\begin{aligned}\delta\tilde{\Pi}_2 = &-\int_{x_A}^{x_B} (N_{xy}\delta u + N_y \delta v)|_{y=W/2}\, dx \\ &+ \int_{y_B}^{y_C} \left(N_x \delta u + N_{xy}\delta v\right)|_{x=-L/2}\, dy \\ &- \int_{x_C}^{x_D} (N_{xy}\delta u + N_y \delta v)|_{y=-W/2}\, dx \\ &+ \int_{y_D}^{y_A} \left[\left(N_x - \frac{P}{W}\right)\delta u + N_{xy}\delta v\right]\Big|_{x=L/2} dy \\ &- \sum_{i=1}^{m} \left\{ \int_{-\pi/2}^{\pi/2} \left(N_r^i \delta u_r^i + N_{r\theta}^i \delta u_\theta^i\right) r_i\, d\beta \right. \\ &\left. + \int_{-\pi/2}^{3\pi/2} \left[\left(N_r^i - \lambda^i\right)\delta u_r^i - \left(u_r^i - \bar{u}_r^i\right)\delta\lambda^i + N_{r\theta}^i \delta u_\theta^i\right] r_i\, d\beta \right\}\end{aligned} \tag{7}$$

Similarly, only boundary integrations are involved in Eq. (7). To seek the solutions using the formulations in Eqs. (5) and (7), we selected the trial functions for the stress potentials as

$$\begin{aligned}\varphi_1 &= C_{10} + \sum_{n=1}^{N} C_{1n} z_1^n + \sum_{i=1}^{m}\left(D_{10}^i \ell n\, \zeta_{1i} + \sum_{n=1}^{N} D_{1n}^i \zeta_{1i}^{-n}\right) \\ \varphi_2 &= C_{20} + \sum_{n=1}^{N} C_{2n} z_2^n + \sum_{i=1}^{m}\left(D_{20}^i \ell n\, \zeta_{2i} + \sum_{n=1}^{N} D_{2n}^i \zeta_{2i}^{-n}\right)\end{aligned} \tag{8}$$

where $z_k = x + \mu_k y$, $k = 1, 2$, are complex coordinate variables; C_{1n}, D_{1n}^i, C_{2n}, and D_{2n}^i are complex constants to be determined; and the mapping functions are

$$\zeta_{ki} = \frac{z_k \pm \sqrt{z_k^2 - r_i^2\left(1 + \mu_k^2\right)}}{r_i(1 - \mu_k I)}, \qquad k = 1, 2, \qquad i = 1, 2, \ldots, m \tag{9}$$

For the Lagrangian multipliers, the following trigonometric functions are selected:

$$\lambda^i(\beta) = \lambda_1^i + \sum_{j=1}^{J}\left[\lambda_{2j}^i \sin(j\beta) + \lambda_{2j+1}^i \cos(j\beta)\right] \qquad i = 1, 2, \ldots, m \tag{10}$$

For accurate and convergent solutions from the variational formulations, some additional conditions must be imposed. The logarithmic terms in the stress potentials must result in single-valued displacements around each rivet hole. The applied load must be in equilibrium with the compressive stresses at rivet holes represented by the Lagrangian multipliers.

There are $2(m+1)(N+1)$ complex constants in Eq. (8) and $m(J+1)$ real constants in Eq. (10), which are determined by the variational formulations. Once these constants are determined, the stress and displacement components are calculated using Eqs. (1) and (2).

Finite Element Modeling Method

Finite element modeling techniques have been proposed for the purpose of analyzing problems with relatively complicated geometry and loading conditions. A major difficulty in modeling riveted joints is the idealization of the load transfer between the rivet and the plate. The resulting stress distribution around the rivet hole is largely influenced by the procedures followed in the idealization. Therefore several alternative strategies for finite element modeling have been investigated in the present program on multiple site damage in lap joints. For comparison with the analytical method outlined in the preceding section, the two-dimensional modeling method using gap/spring elements is discussed in this section. The commercial finite element packages MSC/PATRAN and MSC/NASTRAN were used for the analyses.

A salient idea in the present modeling method is to simulate the rivet by an assembly of a circular beam and two disks that are rigidly connected at the end of the beam. The thickness of the two disks is equal to that of the two plates, and the geometry of the beam is identical to that of the rivet (countersink is not considered). The two plates with rivet holes and the two end disks of the rivet are modeled by two-dimensional plane stress elements. The rivet itself is modeled by a single beam element. Gap/spring elements are then generated to connect the nodes in the contact region along the rivet/plate boundary. Figure 2 demonstrates a finite element model and the rivet hole representation for a four-rivet single lap joint using 80 gap elements around each rivet hole.

Gap/spring elements are one-dimensional elements that simulate unidirectional point-to-point contact between two media (in the present models the plate and the rivet). Gap elements are appropriate in modeling the load transfer between the rivet and the plate under general loading conditions. This is because gap elements require two

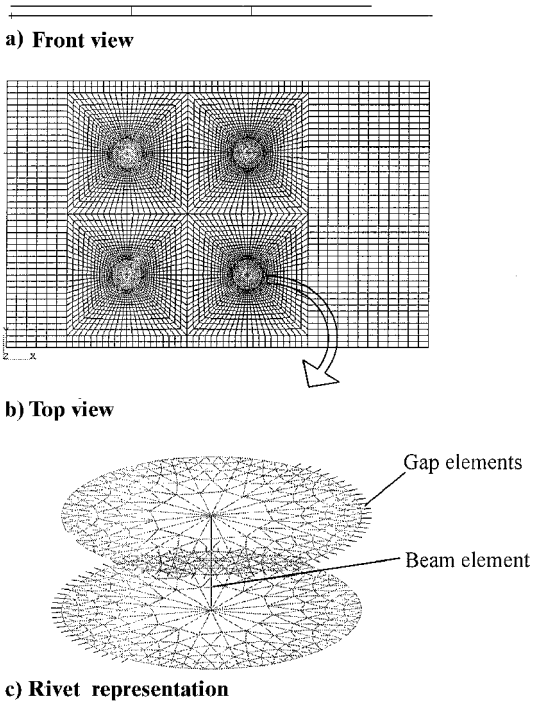

Fig. 2 Finite element model of a four-rivet joint.

separate values of axial stiffness constants: the opening (or tensile) and the closed (or compressive). Two types of nonlinear analyses are usually conducted when using gap elements. One is associated with both the update of the contact region and the large deformation of the whole structure, referred to as nonlinear 1 in this paper. The other, referred to as nonlinear 2, is associated with the update of the contact region only. Spring elements are used only if the contact region is known to be fixed during the loading history as only one stiffness constant is required for spring elements. Linear analyses are usually conducted when using spring elements, as there is no update of the contact region.

A major deficiency when using gap elements is that it requires nonlinear analysis. This may not be desirable if the structure contains a large number of rivets that require much more computational time than that required for the traditional linear analysis. Therefore a good compromise needs to be achieved between the accuracy and the computational efficiency.

A convergence study was conducted to determine the appropriate number of gap/spring elements that would adequately model the load transfer between the rivet and the plates. For simplicity, the analysis was performed for a single rivet joint under a unidirectional load. Linear analysis was done using 30–200 spring elements along one-half of the rivet hole because the load is unidirectional. Nonlinear analysis with large deformation of the whole structure (nonlinear 1) was done in the corresponding models by changing the springs to gap elements. When 200 gap/spring elements are used, the model contains a total of 28,788 degrees of freedom. The degrees of freedom decrease to 6584 for a model with 50 gap/spring elements. Note that as the number of gap/spring elements increases along the rivet hole, the mesh becomes finer in the vicinity of the rivet area. This obviously influences the calculated stress values because the size of the elements around the rivet hole is different for each case.

Figure 3 shows the convergence of the peak stress obtained from linear and nonlinear analyses with varying numbers of gap/spring elements. Apparently, the values obtained by the linear analysis are upper bounds for those by the nonlinear analysis. The change in the peak stress becomes insignificant by increasing the number of gap/springs from about 100 to 200. The numerical values of the peak stress and the CPU time required to run each model are listed in Table 1. The values of the peak stress obtained from the model with 40 gap/spring elements are relatively close to the convergent values, but the CPU time for this model is significantly less than that for the model with 200 gap/spring elements. This indicates that a model with 40–100 gap/spring elements would be a good compromise between the accuracy and the computational efficiency. Therefore 80 gap/spring elements are used in the present finite element models for the example problems discussed next.

Table 1 Stress concentration and CPU time for various models

Number of gaps or springs	Analysis type			
	Spring (linear)		Gap (nonlinear 1)	
	SCF[a]	CPU, s	SCF	CPU, s
30	5.16	18	4.01	72
40	5.20	22	4.18	86
50	5.35	26	4.30	93
100	5.60	32	4.74	151
200	5.73	110	4.97	853

[a]Stress concentration factor.

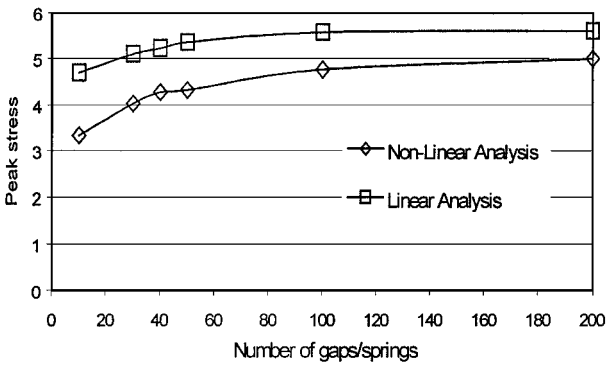

Fig. 3 Convergence of peak stress.

Results and Discussion

Using the analytical and numerical modeling methods outlined earlier, we have analyzed several example problems. Detailed results from the two modeling methods are presented and discussed next.

In the first case, for the purpose of demonstrating the effectiveness of the complex variational approach, a rectangular composite plate AS4/3501-6 $[45/0/-45/0/90/0/45/0/-45/0]_{2s}$ with three loaded holes was analyzed. The dimensions of the plate, as shown in Fig. 4, are $W = 101.6$ mm, $L = 152.4$ mm, $e = 41.2$ mm, $s = 35$ mm, $d_1 = d_3 = 20$ mm, and $d_2 = 30$ mm. A linear finite element analysis was also conducted where the rivets were modeled by a set of stiff spring elements. A comparison of the stress contours in the loading direction from the complex variational approach and the finite element analysis are presented in the upper and lower parts of Fig. 5, respectively, and an excellent agreement is shown.

In the following examples of lap joint geometry configurations, the two plates are aluminum with a thickness of 2.54 mm. All rivet holes have a diameter of 7.9375 mm. Three types of analyses (linear, nonlinear 1, and nonlinear 2) were conducted using the finite element method. The finite element results are compared with those from the analytical method. In the analytical method for multirivet joints,

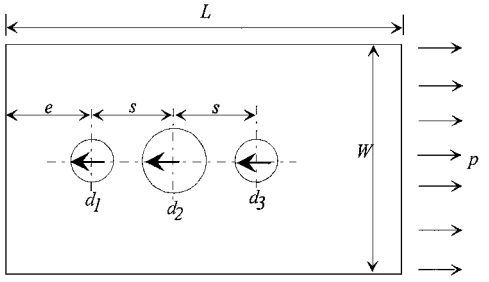

Fig. 4 Composite plate with three loaded holes.

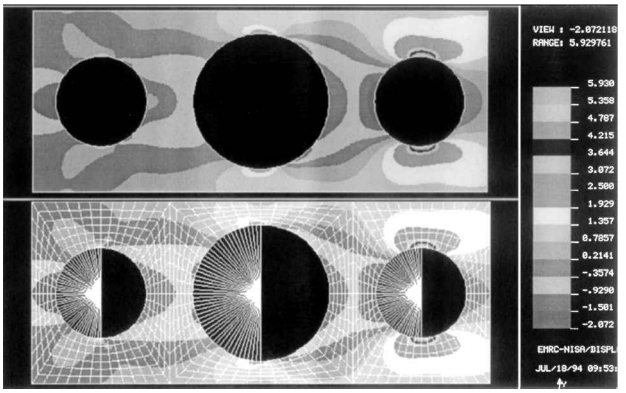

Fig. 5 Stress distributions around three loaded holes (upper: analytical; lower: finite element).

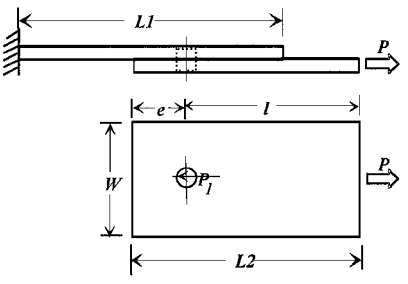

Fig. 6 Single rivet lap joint.

Table 2 Results for a two-rivet lap joint

Method	Quantity	Hole no. 1	Hole no. 2
Analytical	P_i/P	0.49	0.51
	Peak σ_r	−2.51	−2.55
	Peak σ_θ	2.94	4.48
Finite element	P_i/P	0.50	0.50
Linear	Peak σ_r	−2.58	−2.28
	Peak σ_θ	3.38	4.67
Finite element	P_i/P	0.50	0.50
Nonlinear 1	Peak σ_r	−2.62	−2.31
	Peak σ_θ	2.40	3.89
Finite element	P_i/P	0.50	0.50
Nonlinear 2	Peak σ_r	−2.59	−2.28
	Peak σ_θ	2.87	4.55

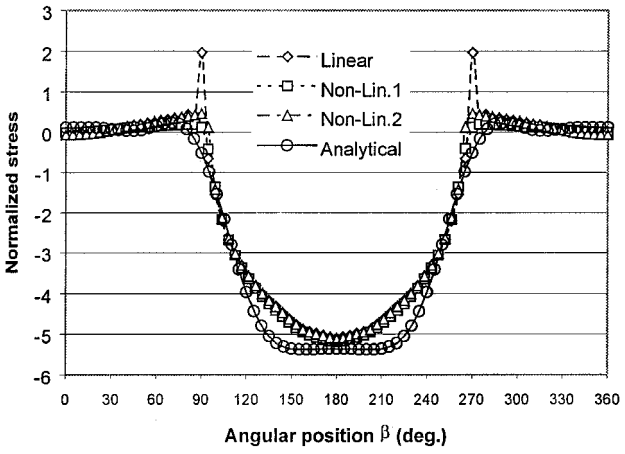

Fig. 7 Bearing stress around rivet hole.

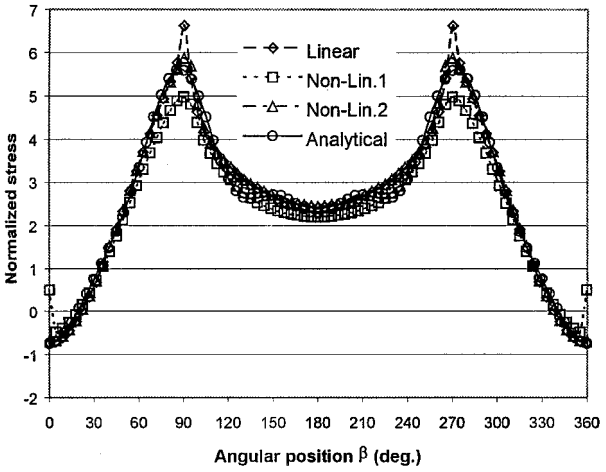

Fig. 8 Hoop stress around rivet hole.

three complex and six real terms were taken in each stress potential and each Lagrangian multiplier, respectively.

The stress values around rivet holes are of importance in strength prediction of lap joints. A single rivet joint, as shown in Fig. 6, was analyzed in the second case by the analytical method, with six terms in each stress potential, and by the finite element method. In this joint, $L_1 = 63.5$ mm, $L_2 = 79.375$ mm, $W = 38.1$ mm, and $e = 31.75$ mm. The distributions of the hoop and bearing stresses around the rivet hole in plate 2, normalized with respect to the far-field stress, are shown in Figs. 7 and 8, respectively. It is seen that the overall distributions from the analytical method and the three types of finite element analyses agree very well. The high peak values from the linear analysis are due to the discontinuity of stiffness at the junctures of the contact and noncontact regions. It is therefore

Table 3 Results for a four-rivet lap joint

Method	Quantity	Hole no. 1	2	3	4
Analytical	P_i/P	0.25	0.25	0.25	0.25
	Peak σ_r	−2.32	−2.32	−2.66	−2.66
	Peak σ_θ	2.91	2.91	4.29	4.29
Finite element	P_i/P	0.25	0.25	0.25	0.25
Linear	Peak σ_r	−2.38	−2.38	−2.22	−2.22
	Peak σ_θ	3.24	3.24	5.19	5.19
Finite element	P_i/P	0.25	0.25	0.25	0.25
Nonlinear 1	Peak σ_r	−2.42	−2.42	−2.27	−2.27
	Peak σ_θ	2.31	2.31	3.79	3.79
Finite element	P_i/P	0.25	0.25	0.25	0.25
Nonlinear 2	Peak σ_r	−2.39	−2.39	−2.22	−2.22
	Peak σ_θ	2.73	2.73	4.47	4.47

Table 4 Results for a five-rivet lap joint

Method	Quantity	Hole no. 1	2	3	4	5
Analytical	P_i/P	0.28	0.16	0.12	0.15	0.30
	Peak σ_r	−1.46	−0.88	−0.67	−1.04	−1.54
	Peak σ_θ	1.60	1.77	1.78	2.63	3.48
Finite element	P_i/P	0.31	0.14	0.10	0.14	0.31
Linear	Peak σ_r	−1.58	−0.68	−0.61	−0.79	−1.49
	Peak σ_θ	2.07	1.80	1.98	2.50	4.01
Finite element	P_i/P	0.31	0.14	0.10	0.14	0.31
Nonlinear 1	Peak σ_r	−1.59	−0.71	−0.64	−0.83	−1.52
	Peak σ_θ	1.49	1.55	1.73	2.19	3.46
Finite element	P_i/P	0.31	0.14	0.10	0.14	0.31
Nonlinear 2	Peak σ_r	−1.57	−0.69	−0.62	−0.80	−1.48
	Peak σ_θ	1.77	1.80	1.99	2.51	4.00

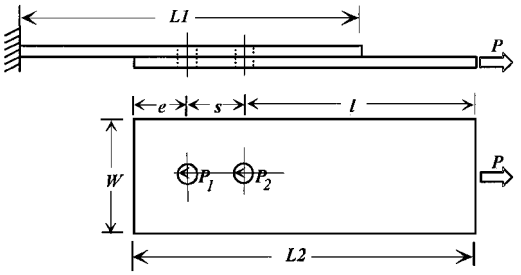

Fig. 9 Two-rivet lap joint.

concluded that linear finite element analysis using spring elements is not appropriate for determining peak stresses.

The second lap joint analyzed was one with two rivets as shown in Fig. 9. In this joint, $L_1 = 95.25$ mm, $L_2 = 111.125$ mm, $W = 38.1$ mm, and $e = 31.75$ mm. The rivet loads, peak bearing stress, and peak hoop stress calculated from the analytical and finite element methods are presented in Table 2. It is seen that the analytical results are in close agreement with the finite element data, particularly with those from the nonlinear analysis in which the nonlinearity is only associated with the update of the gaps' opening and closing (nonlinear 2).

A third lap joint, containing four rivets as shown in Fig. 10, was analyzed. In this joint, $L_1 = 95.25$ mm, $L_2 = 111.125$ mm, $W = 69.85$ mm, $e = 31.75$ mm, and $s = 31.75$ mm. The rivet loads, peak bearing stress, and peak hoop stress calculated from the analytical and finite element methods are presented in Table 3. Similar agreement between the analytical results and the finite element data is noted as in the two-rivet joint.

The last lap joint analyzed was one containing five rivets as shown in Fig. 11. In this joint, $L_1 = 190.5$ mm, $L_2 = 206.375$ mm, $W = 38.1$ mm, $e = 31.75$ mm, and $s = 31.75$ mm. The rivet loads, peak bearing stress, and peak hoop stress calculated from the analytical and finite element methods are presented in Table 4. Similar agreement between the analytical results and the finite element data is also noted as in the two-rivet and four-rivet joints. To show the

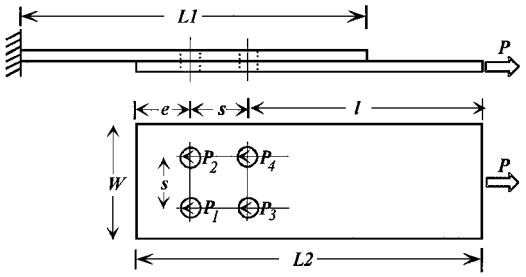

Fig. 10 Four-rivet lap joint.

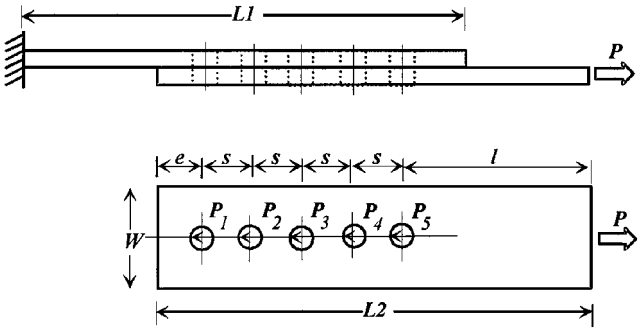

Fig. 11 Five-rivet lap joint.

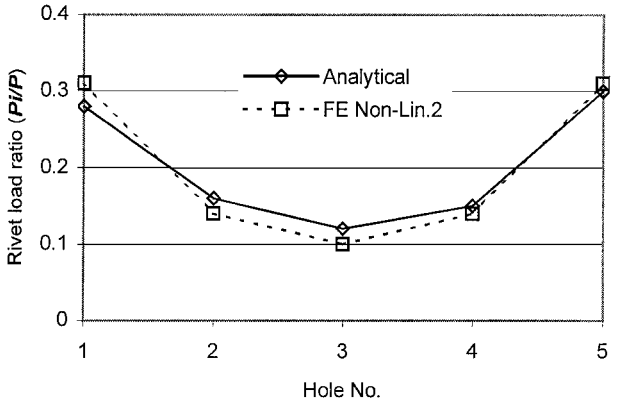

Fig. 12 Rivet loads in five-rivet joint.

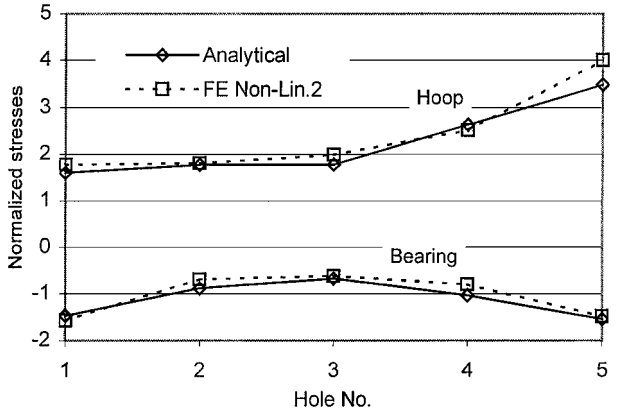

Fig. 13 Peak stresses in five-rivet joint.

comparisons in a graphical form, the rivet loads and peak stresses in this joint are displayed in Figs. 12 and 13, respectively.

Conclusions

Analytical methods have been developed based on the complex variational approach for lap joints with single or multiple rivet holes. The joined plates can be either metallic or composite materials. The stresses in the two joined plates and the rivet loads can be determined. There is no need for finite width correction factors when the rivet holes are not small compared with the width of the joined plates, for example, when the ratio between plate width and hole diameter is less than four. An iterative procedure is implemented to take into account the flexibility of all of the joined members.

Finite element simulations have also been carried out with the following objectives: 1) to verify the analytical methods developed and 2) to explore effective modeling procedures to simulate the rivet–hole interactions. Both gap and spring elements were used, and the effects of these elements on the load transfer were examined. Particularly, the results using different numbers of gap/spring elements around rivet holes were evaluated from the points of view of computational efficiency and accuracy. Comparisons between the results from the analytical and the finite element modeling procedures were presented and discussed.

Based on the results discussed, the following conclusions can be drawn:

1) The analytical method developed using the complex variational approach is efficient for determining the stresses in multirivet lap joints under a unidirectional load, as demonstrated by comparing the results with the finite element calculations. Preliminary design work can be carried out using the analytical method programmed in a personal computer environment. Further development work can be conducted to extend the capability of the analytical method to deal with multirivet joints under general loading conditions.

2) The two-dimensional finite element modeling technique using gap/spring elements is an effective way to analyze riveted lap joints with relatively complicated geometry and loading conditions.

3) The rivet representation by an elastic beam with two end disks is appropriate, and approximately 40–100 gap/spring elements along the contact region are sufficient for adequate accuracy and efficiency.

4) The linear analysis using spring elements predicts accurate overall stress distributions in the joint, but it is not appropriate for determining the peak stresses at the junctures between the contacting and noncontacting regions.

5) The nonlinear analysis associated with both the update of gap elements and the large deformation of the whole structure provides the lower bounds for the peak stresses. This analysis requires the most extensive computing time.

6) The nonlinear analysis associated with the update of gap elements only provides the peak stresses, which are between the values calculated from the linear analysis and the complete nonlinear analysis (nonlinear 1). Also the computing time required by this type of nonlinear analysis is significantly less than that required by nonlinear 1. Therefore it is recommended to use this type of nonlinear analysis with 40–100 gap elements in future finite element modeling of riveted lap joints.

Acknowledgments

This work has been carried out under Institute for Aerospace Research Program 303, Aerospace Structures, Projects SAA-00 and SAB-00, Computational Structures Technology Development. The financial assistance received from Department of National Defence CRAD Funding (FE#1450VA 3GB12 101A 7298) is gratefully acknowledged.

References

[1]Jones, R., and Miller, N. J. (eds.), *Proceedings of International Conference on Aircraft Damage Assessment and Repair*, Inst. of Engineering, Melbourne, Australia, 1991.

[2]Poon, C., and Xiong, Y., "Bolted Joint Technology in Composite Structures—Analytical Tools Development," *Bolted/Bonded Joints in Polymeric Composites* (Florence, Italy), CP-590, AGARD, 1996.

[3]Eastaugh, G., Simpson, D. L., Straznicky, P., and Wakeman, R. B., "A Special Uniaxial Coupon Test Specimen for Simulation of Multiple Site Fatigue Crack Growth and Link-Up in Fuselage Skin Splices," CP-568, AGARD, May 1995.

[4]Lekhnitskii, S. G., *Anisotropic Plates*, Gordon and Breach, New York, 1968, Chap. 6.

[5]De Jong, T., "Stresses Around Pin-Loaded Holes in Elastically Orthotropic or Isotropic Plates," *Journal of Composite Materials*, Vol. 11, July 1977, pp. 313–331.

[6]Zhang, K. D., and Ueng, C. E. S., "Stresses Around a Pin-Loaded Hole in Orthotropic Plates with Arbitrary Loading Direction," *Composite Structures*, Vol. 3, No. 2, 1985, pp. 119–143.

[7]Garbo, S. P., and Ogonowski, J. M., "Effect of Variances and Manufacturing Tolerances on the Design Strength and Life of Mechanically Fastened Composite Joints, I. Methodology Development and Data Evaluation," U.S. Air Force Wright Aeronautical Lab., AFWAL-TR-81-3041, Wright–Patterson AFB, OH, April 1982.

[8]Bowie, O. L., and Neal, D. M., "A Modified Mapping-Collocation Technique for Accurate Calculation of Stress Intensity Factors," *International Journal of Fracture Mechanics*, Vol. 6, No. 2, 1970, pp. 199–206.

[9]Madenci, E., and Ileri, L., "Analytical Determination of Contact Stresses in Mechanically Fastened Composite Laminates with Finite Boundaries," *International Journal of Solids and Structures*, Vol. 30, No. 18, 1993, pp. 2469–2484.

[10]Tong, P., Greif, R., and Chen, L., "Residual Strength of Aircraft Panels with Multiple Site Damage," *Computational Mechanics*, Vol. 13, 1994, pp. 285–294.

[11]Xiong, Y., "An Analytical Method for Failure Prediction of Multi-Rivet Composite Joints," *International Journal of Solids and Structures*, Vol. 33, 1996, pp. 4395–4409.

[12]Waszczak, J. P., and Cruse, T. A., "Failure Mode and Strength Predictions of Anisotropic Bolt Bearing Specimens," *Journal of Composite Materials*, Vol. 5, 1971, pp. 421–425.

[13]Crews, J. H., Jr., Hong, C. S., and Raju, I. S., "Stress-Concentration Factors for Finite Orthotropic Laminates with a Pin-Loaded Hole," NASA TP 1862, 1981.

[14]Chang, F.-K., Scott, R. A., and Springer, G. S., "Strength of Bolted Joints in Laminated Composites," U.S. Air Force Wright Aeronautical Lab., AFWAL-TR-84-4029, Wright–Patterson AFB, OH, 1984.

[15]Roach, D. P., and Jeong, D. Y., "Experimental and Analytical Program to Determine Strains in 737 Lap Splice Joints Subjected to Normal Fuselage Pressurization Loads," AIAA Paper 96-1558, 1996.

[16]Beuth, J. L., and Hutchinson, J. W., "Fracture Analysis of Multi-Site Cracking in Fuselage Lap Joints," *Computational Mechanics*, Vol. 13, 1994, pp. 315–331.

[17]Fung, C.-P., and Smart, J., "Riveted Single Lap Joints, Part 1: A Numerical Parametric Study," *Proc. Instn. Mech. Engrs.*, Vol. 211, Pt. G, 1997, pp. 13–27.

[18]Bellinger, N. C., Krishnakumar, S., and Komorowski, J. P., "Modeling of Pillowing due to Corrosion in Fuselage Lap Joints," *Canadian Aeronautics and Space Journal*, Vol. 40, No. 3, 1994, pp. 125–130.

A. Chattopadhyay
Associate Editor